Journal of Power Sources 195 (2010) 3084–3090

Contents lists available at ScienceDirect

Journal of Power Sources

journal homepage: www.elsevier.com/locate/jpowsour

Conceptual design of a novel ammonia-fuelled portable solid oxide fuel cell system

Siamak Farhad [a], Feridun Hamdullahpur [b,*]

[a] Department of Mechanical & Aerospace Engineering, Carleton University, 1125 Colonel By Dr., Ottawa, ON, Canada K1S 5B6
[b] Department of Mechanical & Mechatronics Engineering, University of Waterloo, 200 University Avenue West Waterloo, ON, Canada N2L 3G1

ARTICLE INFO

Article history:
Received 14 October 2009
Received in revised form
22 November 2009
Accepted 25 November 2009
Available online 1 December 2009

Keywords:
Solid oxide fuel cell
Ammonia fuel
Portable system
Electric power generation
Performance evaluation
Conceptual design

ABSTRACT

A novel portable electric power generation system, fuelled by ammonia, is introduced and its performance is evaluated. In this system, a solid oxide fuel cell (SOFC) stack that consists of anode-supported planar cells with Ni–YSZ anode, YSZ electrolyte and YSZ–LSM cathode is used to generate electric power. The small size, simplicity, and high electrical efficiency are the main advantages of this environmentally friendly system. The results predicted through computer simulation of this system confirm that the first-law efficiency of 41.1% with the system operating voltage of 25.6 V is attainable for a 100 W portable system, operated at the cell voltage of 0.73 V and fuel utilization ratio of 80%. In these operating conditions, an ammonia cylinder with a capacity of 0.8 l is sufficient to sustain full-load operation of the portable system for 9 h and 34 min. The effect of the cell operating voltage at different fuel utilization ratios on the number of cells required in the SOFC stack, the first- and second-law efficiencies, the system operating voltage, the excess air, the heat transfer from the SOFC stack, and the duration of operation of the portable system with a cylinder of ammonia fuel, are also studied through a detailed sensitivity analysis. Overall, the ammonia-fuelled SOFC system introduced in this paper exhibits an appropriate performance for portable power generation applications.

1. Introduction

Solid oxide fuel cells (SOFCs) are power generation devices that can convert chemical energy of a variety of fuels, such as hydrogen, hydrocarbons, ammonia, and biomass, into electrical energy with high efficiency and low environmental impact. The SOFCs are suitable for power generation from a few watts to many megawatts in distributed and centralized applications. The portable application of SOFCs has been recently increased [1–3]; however, selecting a proper fuel is a crucial step for its commercialization. Such a fuel should be cheap, safe, and easy to store and transport. Hydrogen is both expensive and difficult to store and transport [4]. To use hydrocarbon fuels, a fuel processor to prevent carbon deposition over the anode catalyst and a gas clean-up system to separate sulfur compounds from the fuel are usually required [5,6]; hence, the size and cost of the portable system increases. For the following reasons, ammonia can be considered as an adequate substitute for hydrogen and hydrocarbon fuels for portable application of SOFC-based power generation systems [7–10]:

- At ambient temperature and pressure of around 10 atm, the gaseous ammonia is liquefied and its density increases by approximately 850 times, which makes it a cost-effective fuel for transportation and storage. In this condition, the volumetric energy density of the ammonia is comparable with that of gasoline or methanol [11].
- Ammonia can be produced in massive quantities at a cost as competitive as hydrocarbon fuels [7], and its cost per volume of stored energy is approximately 3 times less than that of hydrogen [12].
- Ammonia is safer than hydrogen and hydrocarbon fuels because it does not burn in air under normal conditions, and as such is considered non-flammable when transported. If ammonia is released into the atmosphere, it dissipates rapidly and because of its distinct smell, can easily be detected by the human nose [13].
- According to the results of fuel maps developed for SOFCs, ammonia is a suitable fuel for electric power generation with high maximum voltage and electrical efficiency [14,15].

Of course, ammonia is corrosive [16]. If it is directly fed to an oxygen ion conducting SOFC, the anode catalyst is rapidly destroyed. This problem can be solved by decomposing ammonia into its constituent elements, i.e. nitrogen and hydrogen, before feeding it to the SOFC stack in the portable system. The corrosion problem of

* Corresponding author. Tel.: +1 519 888 4766; fax: +1 519 885 5862.
E-mail addresses: siamak.farhad@yahoo.com (S. Farhad), fhamdull@uwaterloo.ca (F. Hamdullahpur).

0378-7753/$ – see front matter © 2009 Elsevier B.V. All rights reserved.
doi:10.1016/j.jpowsour.2009.11.115

Nomenclature

C_p	heat capacity at constant pressure (kJ kg^{-1} K^{-1})
$\dot{E}x$	exergy (W)
k	heat capacity ratio
LHV	lower heating value (kJ kg^{-1})
$\dot{m}$	mass flow rate (kg s^{-1})
p	pressure (Pa)
T	temperature (K)
U_f	fuel utilization ratio (%)
$\dot{W}$	electric power (W)

Greek letters

η	efficiency

Subscripts

I	first law of thermodynamic
II	second law of thermodynamic

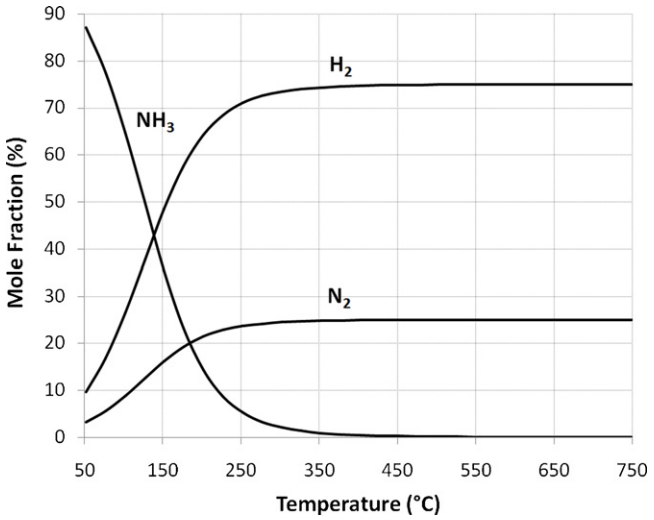

Fig. 2. Mole fraction of ammonia, hydrogen and nitrogen in thermodynamic equilibrium at different temperatures.

ammonia in other components of a portable system can also be solved by selecting a suitable alloy with an appropriate thickness for these components [17].

Introducing and conceptually designing a novel ammonia-fuelled portable power generation system using the oxygen ion conducting SOFC are the purposes of this study.

2. System description

The configuration of the portable SOFC system is shown in Fig. 1. The system is mainly comprised of an oxygen ion conducting SOFC stack to produce DC electricity; liquid ammonia and water cylinders, enough for a specified-duration of operation of the portable system; an air blower to supply air to the SOFC stack and to overcome the pressure drop in the system; a heat exchanger to increase the temperature of air, water and ammonia before entering the SOFC stack; and a catalytic burner to convert the chemical energy of the unutilized fuel in the SOFC stack to heat. In contrast to hydrocarbon-fuelled SOFC systems, a clean-up component to remove sulfur compounds from the fuel is not required. Even if the hydrogen required to produce ammonia is obtained from fossil or renewable fuels, the sulfur compounds are removed from the feedstock in the first step of the ammonia production process, because sulfur compounds deactivate catalysts used in this process [18].

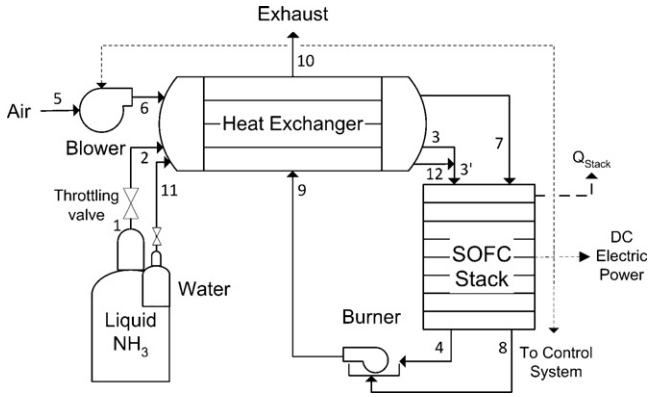

Fig. 1. Configuration of the introduced ammonia-fuelled portable SOFC system.

3. Process description

The pressurized liquid ammonia in the small cylinder is vaporized using a throttle valve. Although direct utilization of the vaporized ammonia in proton conducting SOFCs is possible [19–25], the ammonia content of the inlet fuel to an oxygen ion conducting SOFC should be kept as low as possible to prevent the corrosion problem. In the portable SOFC system illustrated in Fig. 1, the vaporized ammonia enters a heat exchanger where its temperature increases to around 700 °C. By increasing the temperature, the ammonia begins to decompose into its constituent elements, i.e. hydrogen and nitrogen, through the following endothermic reaction [26]:

$$NH_3 + 46.5\,\text{kJ mol}^{-1} \leftrightarrow 1.5H_2 + 0.5N_2 \quad \text{(R1)}$$

To predict the composition of the ammonia at the outlet of the heat exchanger, a thermodynamic equilibrium-based study was performed, and the result is shown in Fig. 2. As shown in this figure, for temperatures higher than 450 °C, more than 99% of the ammonia can be decomposed into its constituent elements; however, the rate of the decomposition reaction is slow at this temperature [27]. The amount of ammonia at the inlet of the SOFC stack can reach less than 250 ppm in equilibrium at a temperature of 700 °C. It is assumed that the ammonia decomposition reaction is fast enough at this temperature compared to the residence time of ammonia in the heat exchanger. Because iron acts as a suitable catalyst for the ammonia decomposition reaction [28,29], an iron porous body can be also inserted in the ammonia's paths in the heat exchanger to increase the rate of the reaction. In this condition, the outlet fuel from the heat exchanger will be in thermodynamic equilibrium.

The temperatures of the outlet water from the water cylinder and the pressurized air in the blower also increase to 700 °C in the heat exchanger. The water vapour at 700 °C is then mixed with the decomposed ammonia and a suitable fuel for the SOFC stack is prepared. The fuel and air enter the SOFC stack where the electric power, heat and water vapour are generated due to the electrochemical reaction of hydrogen and oxygen. Ma et al. [7] investigated the possibility of nitric oxide formation in a variety of ammonia conversion rates and temperatures in SOFCs. They found that the amount of nitric oxide is not detectable even at 800 °C. Therefore, nitric oxide is not expected to be formed in the SOFC stack of the ammonia-fuelled portable system. The outlet fuel and air from the SOFC stack enter a catalytic burner where the chemical energy of

the unutilized fuel is converted to heat. A portion of the heat produced in the catalytic burner and SOFC stack is used to increase the temperature of the ammonia, air and water to 700 °C in the heat exchanger, and for the decomposition of ammonia. The remaining heat is vented into the atmosphere with the exhaust gas, which is expected to consist of only water vapour, oxygen and nitrogen.

4. Computer simulation of the portable SOFC system

To evaluate the performance of the portable system, a computer code, developed by the authors for the simulation of planar SOFCs at cell, stack and system levels, was used.

A detailed model of the cell including the electrochemical reactions (R2) and (R3) in the anode and cathode, respectively, was considered in the computer code to determine the activation, ohmic, and concentration polarizations. The modeling of polarizations used in the computer code has been described in Refs. [30–32]. In the cell modeling, the inlet and outlet fuel streams from the anode were assumed to be in thermodynamic equilibrium:

$$H_2 + O^{2-} \rightarrow H_2O + 2e^- \quad \text{(R2)}$$

$$(1/2)O_2 + 2e^- \rightarrow O^{2-} \quad \text{(R3)}$$

The SOFC stack model used in the computer code is the extension of the cell model by taking account of the heat transfer from the SOFC stack. Heat transfer from the SOFC stack affects cell performance, and accordingly, the performance of the portable SOFC system changes. Therefore, a suitable insulation system is required to control the heat transfer. For portable applications of SOFCs, the insulation system should be thin so as to reduce the size of the system. Therefore, a vacuum layer, mechanically supported by two metal layers, is considered for the insulation system of the SOFC stack. In the vacuum layer there can be no conductive or convective heat transfer, and the radiative heat transfer can be minimized by applying a reflective coating on the metal surfaces. To determine the rate of heat transfer from the SOFC stack, radiative heat transfer from the vacuum layer and radiative and natural convective heat transfer from the outer metal layer were taken into account. The effect of heat transfer from the SOFC stack on the cell's performance was finally considered in the computer code. In the stack modeling, a 5% voltage drop in the SOFC stack is assumed.

The balance of plant (BoP) components such as heat exchanger, blower, and catalytic burner was thermodynamically modeled under steady state operating conditions. The properties, composition and flow rate of all streams in the portable system are determined after modeling the BoP components. Finally, the first-law and second-law efficiencies and total exergy destruction of the system is determined from Eqs. (1)–(3), respectively:

$$\eta_{\mathrm{I}} = \frac{\dot{W}_{SOFC\,stack} - \dot{W}_{blower} - \dot{W}_{control\,system}}{\dot{m}_{liquid\,ammonia} LHV_{liquid\,ammonia}} \quad (1)$$

$$\eta_{\mathrm{II}} = \frac{\dot{W}_{SOFC\,stack} - \dot{W}_{blower} - \dot{W}_{control\,system}}{\dot{E}x_{liquid\,ammonia}} \quad (2)$$

$$\dot{E}x_{destruction,total} = \dot{E}x_{liquid\,ammonia} - (\dot{W}_{SOFC\,stack} - \dot{W}_{blower} - \dot{W}_{control\,system}) \quad (3)$$

In these equations, the blower input power can be determined from Eq. (4):

$$\dot{W}_{blower} = \dot{m}_{air} C_{p_{air}} T_5 \left(\left(\frac{p_6}{p_5} \right)^{(k_{air}-1)/k_{air}} - 1 \right) \frac{1}{\eta_{blower}} \quad (4)$$

In the system modeling, the heat transfer from the heat exchanger and catalytic burner was not considered in the calculations.

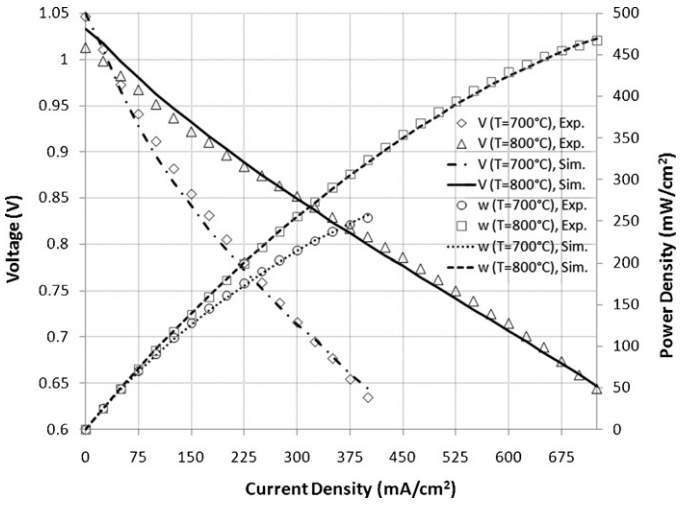

Fig. 3. Results of the computer simulation and experiment for ASC 3 cells.

4.1. Validation of the computer simulation

To validate the computer code at the cell level, we simulated the performance of ASC 3 anode-supported cells, produced by H.C. Starck Company [33]. These cells are comprised of Ni/YSZ (yttrium stabilized zirconia) anode, dense YSZ electrolyte and YSZ/LSM (lanthanum strontium manganese oxide) cathode. The computer code could predict the voltage and power density of this cell at operating temperatures of 700 °C and 800 °C with an average relative error of ±1%. The voltage and power density of ASC 3 cells obtained by the computer simulation and the experiment at various current densities are shown Fig. 3.

4.2. Input data

The input data used for evaluation of the SOFC cell, stack, and the BoP components of the portable system are listed in Tables 1–3, respectively. The ASC 3 cell is used for computer simulation of the SOFC stack. To simulate the ASC 3 cell, it is assumed that the porosity and tortuosity of electrodes are 0.33 and 4, respectively.

In this study, the portable system is generated a net DC electric power of 100 W after deducting the electric power required for the air blower and the control system. For the ammonia cylinder, a capacity of 0.8 l has been taken into consideration.

Table 1
Input data for computer simulation of the cell.

Parameter	Value
Operating temperature	800 °C
Fuel utilization ratio	60%, 70% and 80%
Anode	
Thickness	518 μm
Porosity	0.33
Tortuosity	4
Cathode	
Thickness	45 μm
Porosity	0.33
Tortuosity	4
Electrolyte thickness	5 μm
Interconnect thickness	3000 μm
Cell active length	3 cm
Cell active width	3 cm

Table 2
Input data for computer simulation of the stack.

Parameter	Value
Emissivity of metal surfaces [34]	
Hot surface	0.03
Cold surface	0.01
Emissivity of the outer surface of the SOFC stack	0.8
Fuel inlet temperature	700 °C
Air inlet temperature	700 °C

Table 3
Input data for computer simulation of the portable system.

Parameter	Value
Net DC electric power generation	100 W
Estimated power for control system	20 W
Air blower efficiency	55%
Pressure drop	0.3 bar
Capacity of the ammonia cylinder	0.8 l
Capacity of the water cylinder	30 cm^3
Ammonia to water mixing ratio	19
Heat exchanger pinch temperature	>75 °C

5. Results and discussion

To conceptually design the introduced ammonia-fuelled portable SOFC system, an operating voltage and a fuel utilization ratio should be selected for the cells. To select these parameters, a sensitivity analysis is performed to determine the effects of these parameters on key performance parameters of the portable system.

5.1. Sensitivity analysis

According to the input data presented in Tables 1–3, effects of the cell operating voltage and fuel utilization ratio on the number of cells required in the SOFC stack, the first- and second-law efficiencies, the system operating voltage, the excess air, the heat transfer from the SOFC stack, and duration of operation of the portable system with a full 0.8 l cylinder of ammonia are investigated.

5.1.1. Effect of the cell operating voltage and fuel utilization ratio on the number of cells required in the SOFC stack

As shown in Fig. 4, the number of cells required in the SOFC stack, to generate 100 W net DC electric power, changes parabolically with the cell operating voltage. Based on the cell operating voltage at which the minimum number of cells is obtained, operating voltages of a cell can be divided into two groups [35]. The cell voltages of group I are less, and the cell voltages of group II are more than this voltage. These two groups of cell voltages for the fuel utilization ratio of 80% are shown in Fig. 4.

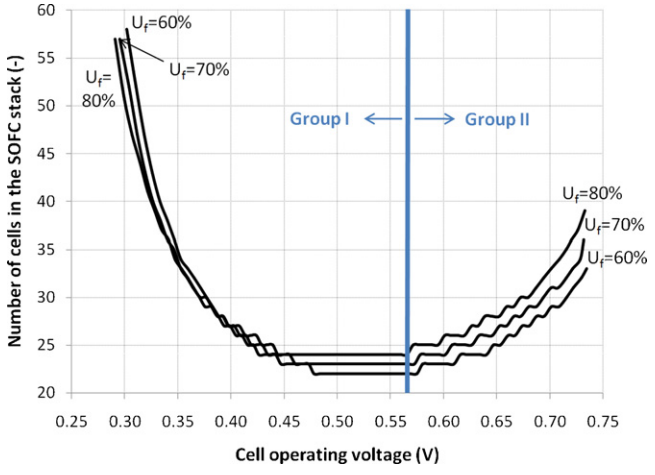

Fig. 4. Effect of the cell operating voltage at fuel utilization ratios of 60%, 70%, and 80% on the number of cells required in the SOFC stack for generating 100 W net electric power in the portable system.

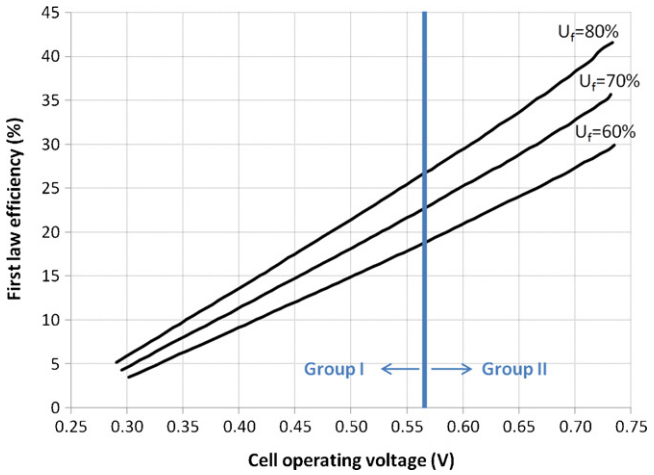

Fig. 5. Effect of the cell operating voltage at fuel utilization ratios of 60%, 70%, and 80% on the first-law efficiency of the portable system.

Fig. 4 shows that the decrease in the cell voltage in group I leads to a sharp increase in the number of cells. Accordingly, the size of the SOFC stack increases that is not suitable for a portable system. The number of cells and size of the SOFC stack reduces with the decrease in the cell voltage in group II. In this group, the number of cells also reduces with the decrease in the fuel utilization ratio. For example, the number of cells reduces by approximately 12% if the fuel utilization ratio reduces from 80% to 60% at the cell operating voltage of 0.7 V.

5.1.2. Effect of the cell operating voltage and fuel utilization ratio on the first- and second-law efficiencies of the portable system

As shown in Figs. 5 and 6, the first- and second-law efficiencies of the portable system increase linearly when the cell operating voltage increases. The cell voltages in group II cause higher first- and second-law efficiencies for the portable system in comparison with cell voltages in group I.

In the range of the fuel utilization ratios investigated, the higher the fuel utilization ratio, the higher the first- and second-law efficiencies. The effect of the fuel utilization ratio on the first- and

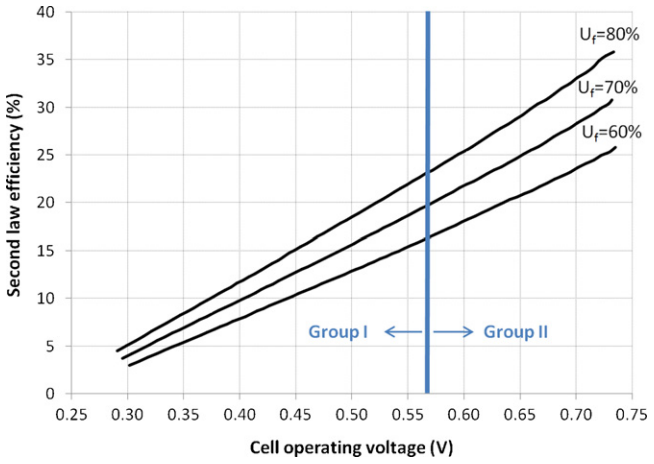

Fig. 6. Effect of the cell operating voltage at fuel utilization ratios of 60%, 70%, and 80% on the second-law efficiency of the portable system.

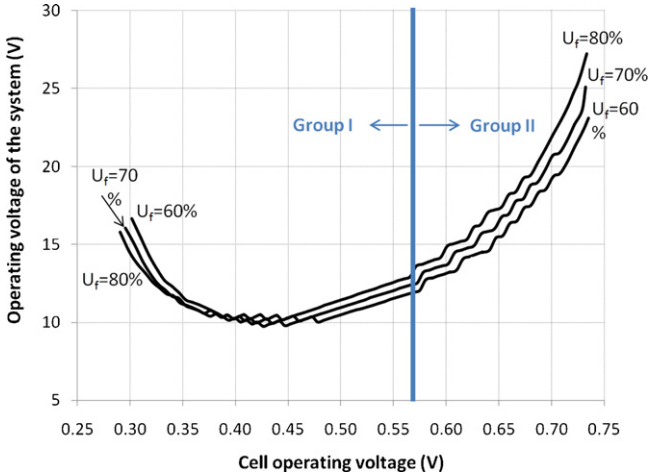

Fig. 7. Effect of the cell operating voltage at fuel utilization ratios of 60%, 70%, and 80% on the operating voltage of the portable system.

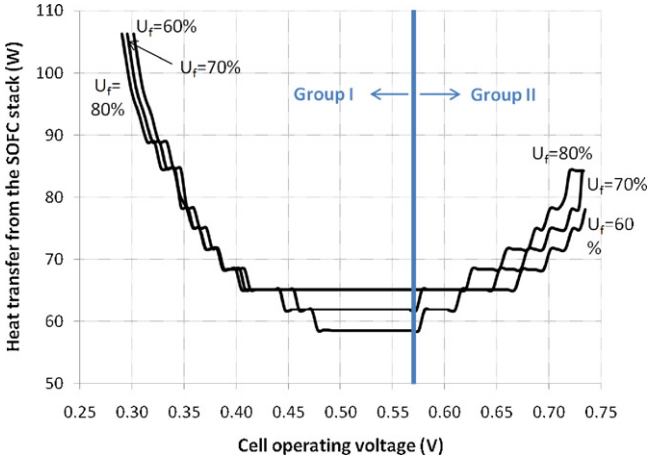

Fig. 9. Effect of the cell operating voltage at fuel utilization ratios of 60%, 70%, and 80% on the amount of heat transfer from the SOFC stack.

second-law efficiencies is more significant at the elevated cell voltages.

5.1.3. Effect of the cell operating voltage and fuel utilization ratio on the system operating voltage

As shown in Fig. 7, the operating voltage of the portable system changes parabolically with the cell operating voltage. Since a high operating voltage for a portable power generation system is usually desirable, selecting a cell operating voltage from the cell voltages of group II may be preferred over selecting voltages from group I. To reach a desired operating voltage for the portable system, the cell operating voltage should be increased in group II or decreased from the cell operating voltage of around 0.44 V in group I.

In group II, the effect of the fuel utilization ratio on the operating voltage of the portable system is significant, especially at the elevated cell operating voltages. For example, the system operating voltage increases by approximately 12% if the fuel utilization ratio increases from 60% to 80% at the cell operating voltage of 0.7 V.

5.1.4. Effect of the cell operating voltage and fuel utilization ratio on the excess air required for the SOFC stack

The effect of the cell operating voltage at fuel utilization ratios of 60%, 70%, and 80% on the excess air, required to control the temperature of the SOFC stack, is shown in Fig. 8. As illustrated in this figure, the increase in the cell operating voltage leads to a decrease in the excess air, and accordingly, the size and cost of the heat exchanger, catalytic burner and air blower in the portable system decreases.

Generally, the higher the fuel utilization ratio, the higher the excess air required for the SOFC stack. However, the effect of the fuel utilization ratio decreases at the elevated cell voltages.

5.1.5. Effect of the cell operating voltage and fuel utilization ratio on the heat transfer from the SOFC stack

As shown in Fig. 9, the amount of the heat transfer from the SOFC stack changes parabolically with the cell operating voltage. The increase of the heat transfer from the SOFC stack leads to a change in the temperature distribution in a cell, and accordingly, the thermal stress in the cell changes. Therefore, it may be important to keep the heat transfer from the SOFC stack as low as possible. As shown in Fig. 9, the minimum amount of the heat transfer occurs at the common boundary of the cell voltages of groups I and II.

The effect of the fuel utilization ratio on the amount of heat transfer from the SOFC stack seems to be significant, especially if the cell operating voltage belongs to group II. For example, the amount of heat transfer decreases by approximately 8% if the fuel utilization ratio decreases from 80% to 60% at the cell operating voltage of 0.7 V.

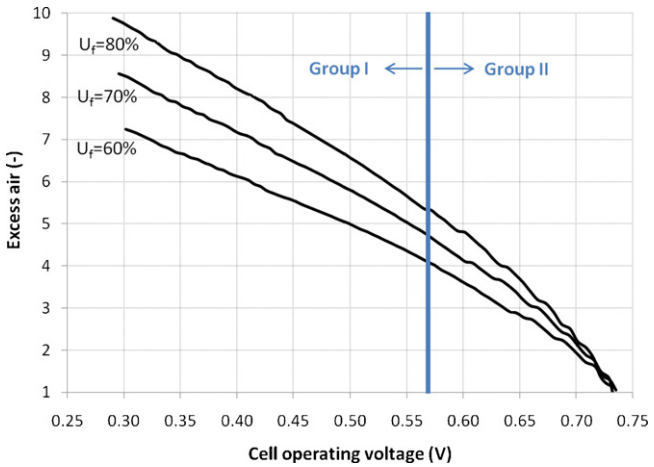

Fig. 8. Effect of the cell operating voltage at fuel utilization ratios of 60%, 70%, and 80% on the excess air required for the SOFC stack.

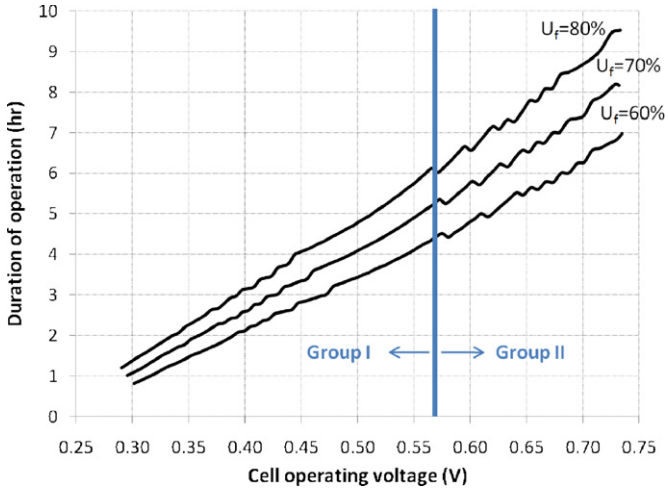

Fig. 10. Effect of the cell operating voltage at fuel utilization ratios of 60%, 70%, and 80% on the duration of operating of the portable system with a full 0.8 l cylinder of ammonia.

Table 4
The computer simulation results for the 100 W ammonia-fuelled portable SOFC system, operated at the cell design voltage of 0.73 V and mCV and fuel utilization ratios of 60%, 70%, and 80%.

Parameter	Fuel utilization ratio (%)			Fuel utilization ratio (%)		
	80	70	60	80	70	60
Cell design voltage (V)	0.73	0.73	0.73	mCV = 0.566	mCV = 0.573	mCV = 0.575
Number of cells required in the SOFC stack	37	34	32	24	23	22
First-law efficiency (%)	41.1	35.1	29.3	26.8	23.2	19.4
Second-law efficiency (%)	35.4	30.3	25.3	23.1	20.0	16.7
Excess air	1.17	1.37	1.32	5.3	4.6	4.0
Duration of operation with a full 0.8 l ammonia cylinder (h:min)	9:34′	8:08′	6:47′	6:07′	5:21′	4:31′
System operating voltage (V)	25.6	23.6	22.2	12.9	12.5	12
Total exergy destruction (W)	157	207	273	316	380	475
Blower input power (W)	6.7	10.3	14	33.0	36.0	40.8

5.1.6. *Effect of the cell operating voltage and fuel utilization ratio on the duration of operation of the portable system*

The duration of operation of the portable system with a full 0.8 l ammonia cylinder at different cell operating voltages and fuel utilizations of 60%, 70%, and 80% is shown in Fig. 10. As shown in this figure, the duration of operation of the portable system increases when the cell operating voltage and fuel utilization ratio increase. The effect of the fuel utilization ratio on the duration of operation is more significant for the cell voltages of group II.

5.2. *The cell design voltage and fuel utilization ratio*

According to the results of the sensitivity analysis, with the decrease in the cell operating voltage in group I, the number of cells and excess air required for the SOFC stack increases. Hence, the size and production cost of the SOFC stack, heat exchanger, air blower, and catalytic burner increase. The decrease in the cell voltage in this group leads also to a decrease in the first- and second-law efficiencies and the duration of operation of the portable system. Therefore, the optimum cell design voltage is not in group I and should be found in the cell voltages of group II. Indeed, the lowest cell operating voltage is limited to the cell voltage at which the minimum number of cells is obtained. This voltage is called the minimum cell voltage (mCV) in this paper. With the increase in the cell voltage in group II, the number of cells required in the SOFC stack increases, accordingly, the size and cost of the SOFC stack increases. Whereas, the increase of the cell operating voltage leads to a significant increase in the duration of operation and operating voltage of the portable system and a significant decrease in the size of the heat exchanger, air blower and catalytic burner due to reduction of the excess air. We selected the cell operating voltage of 0.73 V as the cell design voltage in this study; however, a detailed economic analysis is required to find the optimum cell design voltage.

The key performance parameters of the portable system at the cell voltages of 0.73 V and mCV and fuel utilization ratios of 60%, 70%, and 80% are listed in Table 4. As shown in this table, with the increase of the cell design voltage from the mCV to 0.73 V at the fuel utilization ratio of 60%, the number of cells required in the SOFC stack to generate 100 W net DC electric power in the portable system increases ten cells; however, the first-law efficiency increases from 19.4% to 29.3%, the excess air decreases about 3 times, the duration of operation increases approximately 50%, the system operating voltage increases around 1.85 times, and the electric power required for the air blower reduces around 2.91 times. For the cell design voltage of 0.73 V, if the fuel utilization ratio increases from 60% to 80%, the number of cells required in the SOFC stack increases five cells, although the first-law efficiency increases from 29.3% to 41.1%, the duration of operation increases around 41%, the excess air reduces about 1.13 times, the system operating voltage increases approximately 1.15 times, and the electric power required for the air blower reduces around 2.1 times. Therefore, we selected the fuel utilization ratio of 80% to conceptually design the portable system; however, a detailed economic analysis is required to find the optimum fuel utilization ratio.

If the cell voltage of 0.73 V and fuel utilization ratio of 80% are chosen to conceptually design the introduced ammonia-fuelled portable power generation system, thirty seven cells in the SOFC stack are required to generate 100 W net DC electric power, and the first-law efficiency and the operating voltage of 41.1% and 25.6 V are predicted for the portable system, respectively. It is also expected that a full 0.8 l ammonia cylinder is enough to sustain full-load operation of the system for 9 h and 34 min.

In computer simulations the main source of the error is the assumptions made in both modeling and numerical solution. In the absence of dependable experimental results it is difficult to quantify an error margin. However, considering the qualitative judgment that we made on the validity of our assumptions to simulate the portable system, we suggest a 90% confidence level for results.

5.3. *Exergy analysis*

The share of each component in the portable system in the exergy destruction of the ammonia fuel at the cell voltage of 0.73 V and fuel utilization ratio of 80% is shown in Fig. 11. As illustrated in this figure, around 35.4% of the ammonia's exergy is converted to

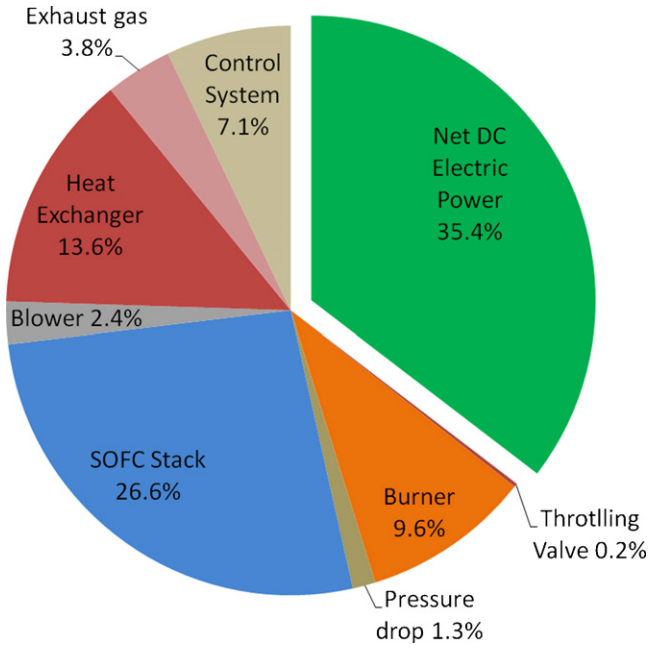

Fig. 11. The share of each component in the portable system in exergy destruction of the ammonia fuel (cell voltage = 0.73 V and U_f = 80%).

electric power in the portable system. Among the different components of the system, the SOFC stack has the largest share in exergy destruction of the ammonia fuel with 26.6%, followed by the heat exchanger with 13.6% and catalytic burner with 9.6%. The exergy analysis also confirm that there is a potential to generate additional electricity if the introduced portable system is combined with other power generation systems such as, a thermoelectric device and appropriately optimized using pinch technology and exergy analysis [36,37].

6. Conclusions

A novel portable SOFC-based power generation system, fuelled by ammonia, was introduced and conceptually designed. This system has a simple layout and its size is small compared to hydrocarbon-fuelled portable SOFC systems. The exhaust gas from the portable system contains only water vapour, oxygen, and nitrogen, and therefore contributes to reduction of greenhouse gases emission. This system also exhibits a high efficiency. If ASC 3 planar cells, operated at the cell voltage of 0.73 V and the temperature of 800 °C are used in the SOFC stack, at the cell fuel utilization ratios of 60%, 70%, and 80%, the first-law efficiency of 29.3%, 35.1%, and 41.1% with the system operating voltage of 22.2 V, 23.6 V, and 25.6 V is expected, respectively, for the portable system. In these conditions, a full 0.8 l ammonia cylinder is sufficient to sustain full-load operation of the portable system for around 6 h and 47 min, 8 h and 8 min, and 9 h and 34 min, respectively. The exergy analysis shows that at the cell design voltage of 0.73 V and the fuel utilization ratio of 80%, around 35.4% of the ammonia's exergy can be converted to electric power in the portable system, and 26.6%, 13.6%, and 9.6% of the ammonia's exergy is destructed in the SOFC stack, heat exchanger, and catalytic burner, respectively. Therefore, there is a potential to generate more electric power if the introduced portable system is combined with other power generation systems such as a thermoelectric device. It was also shown that there is a limitation for selecting a cell voltage at the design stage of the system. Indeed, the minimum cell design voltage is limited to the cell voltage at which the minimum number of cells required in the SOFC stack is obtained. This voltage is dependent on the cell, stack and system design parameters. For the portable system introduced in this paper, the minimum cell voltage of 0.575 V, 0.573 V, and 0.566 V was determined at the cell fuel utilization ratios of 60%, 70%, and 80%, respectively.

Acknowledgment

The authors gratefully acknowledge the financial support provided by Natural Sciences and Engineering Research Council (NSERC) of Canada.

References

[1] H. Hayashi, O. Yamamoto, H. Minoura, Solid State Ionics 132 (2000) 343–345.
[2] Adaptive Materials Inc., www.adaptivematerials.com/ (accessed January 2009).
[3] P.K. Cheekatamarla, C.M. Finnerty, C.R. Robinson, S.M. Andrews, J.A. Brodie, Y. Lu, P.G. DeWald, J. Power Sources 193 (2009) 797–803.
[4] M. Younessi-Sinaki, E.A. Matida, F. Hamdullahpur, Int. J. Hydrogen Energy 34 (2009) 3710–3716.
[5] S. Farhad, Y. Yoo, F. Hamdullahpur, Proceedings of the 9th International Colloquium on Environmentally Preferred Advanced Power Generation (ICEPAG-2009), CA, USA, February, 2009.
[6] S. Farhad, Y. Yoo, F. Hamdullahpur, European Fuel Cell Forum, Lucerne, Switzerland, 2009.
[7] Q. Ma, R.R. Peng, L. Tian, G. Meng, Electrochem. Commun. 8 (2006) 1791–1795.
[8] A. Wojcik, H. Middleton, I. Damopoulos, J. Van herle, J. Power Sources 118 (2003) 342–348.
[9] G.G.M. Fournier, I.W. Cumming, K. Hellgardt, J. Power Sources 162 (2006) 198–206.
[10] A. Fuerte, R.X. Valenzuela, M.J. Escudero, L. Daza, J. Power Sources 192 (2009) 170–174.
[11] C. Zamfirescu, I. Dincer, J. Power Sources 185 (2008) 459–465.
[12] J.O. Jensen, A.P. Vestbo, Q. Li, N.J. Bjerrum, J. Alloys Compd. 446 (2007) 723–728.
[13] J.J. Mackenzie, W.H. Avery, Energy Conversion Engineering Conference, Washington, DC, 1996.
[14] S. Farhad, F. Hamdullahpur, J. Power Sources 191 (2009) 407–416.
[15] S. Farhad, F. Hamdullahpur, J. Power Sources 193 (2009) 632–638.
[16] A.S. Osered'ko, J. Mater. Sci. 15 (1980) 647–649.
[17] G.Y. Lai, High-temperature Corrosion and Materials Applications, ASM International Materials Park, Ohio, 2007, 44073-0002.
[18] W. Arabczyk, D. Moszyński, U. Narkiewicz, R. Pelka, M. Podsiadły, Catal. Today 124 (2007) 43–48.
[19] M. Ni, D.Y.C. Leung, M.K.H. Leung, J. Power Sources 183 (2008) 682–686.
[20] Q. Ma, J. Ma, S. Zhou, R. Yan, J. Gao, G. Meng, J. Power Sources 164 (2007) 86–89.
[21] N. Maffei, L. Pelletier, A. McFarlan, J. Power Sources 175 (2008) 221–225.
[22] N. Maffei, L. Pelletier, J.P. Charland, A. McFarlan, J. Power Sources 162 (2006) 165–167.
[23] K. Xie, Q. Ma, B. Lin, Y. Jiang, J. Gao, X. Liu, G. Meng, J. Power Sources 170 (2007) 38–41.
[24] R. Metkemeijer, P. Achard, J. Power Sources 49 (1994) 271–282.
[25] R. Metkemeijer, P. Achard, Int. J. Hydrogen Energy 19 (1994) 535–542.
[26] J.P. Collins, J.D. Way, J. Membr. Sci. 96 (1994) 259–274.
[27] L. Li, J.A. Hurley, Int. J. Hydrogen Energy 32 (2007) 6–10.
[28] R. Pelka, I. Moszyńska, W. Arabczyk, Catal. Lett. 128 (2009) 72–76.
[29] S.F. Yin, B.Q. Xu, X.P. Zhou, C.T. Au, Appl. Catal. A 277 (2004) 1–9.
[30] S.H. Chan, K.A. Khor, Z.T. Xia, J. Power Sources 93 (2001) 130–140.
[31] A.V. Virkar, J. Chen, C.W. Tanner, J. Kim, Solid State Ionics 131 (2000) 189–198.
[32] J.W. Kim, A.V. Virkar, K.Z. Fung, K. Mehta, S.C. Singhal, J. Electrochem. Soc. 146 (1) (1999) 69–78.
[33] H.C. Starck Company, www.hcstarck-ceramics.com/ (accessed April 2009).
[34] OMEGA Engineering, Inc., www.omega.com/literature/transactions/volume1/emissivitya.html (accessed August 2009).
[35] S. Farhad, F. Hamdullahpur, J. Power Sources 195 (2010) 1446–1453.
[36] S. Farhad, M. Saffar-Avval, M. Younessi-Sinaki, Int. J. Energy Res. 32 (2007) 1–11.
[37] S. Farhad, M. Younessi-Sinaki, M.R. Golriz, F. Hamdullahpur, Int. J. Exergy 5 (2008) 164–176.